PHYSICAL REVIEW D **76,** 084019 (2007)

Gravitational wave spectrum induced by primordial scalar perturbations

Daniel Baumann,[1,*] Paul Steinhardt,[1,2,†] and Keitaro Takahashi[1,‡]

[1]*Department of Physics, Jadwin Hall, Princeton University, Princeton, New Jersey 08544, USA*

[2]*Princeton Center for Theoretical Physics, Jadwin Hall, Princeton University, Princeton, New Jersey 08544, USA*

Kiyotomo Ichiki[§]

Research Center for the Early Universe, University of Tokyo, 7-3-1 Hongo, Bunkyo-ku, Tokyo 113-0033, Japan

(Received 9 June 2007; published 17 October 2007)

We derive the complete spectrum of gravitational waves induced by primordial scalar perturbations ranging over all observable wavelengths. This scalar-induced contribution can be computed directly from the observed scalar perturbations and general relativity and is, in this sense, independent of the cosmological model for generating the perturbations. The spectrum is scale invariant on small scales, but has an interesting scale dependence on large and intermediate scales, where scalar-induced gravitational waves do *not* redshift and are hence enhanced relative to the background density of the Universe. This contribution to the tensor spectrum is significantly different in form from the direct model-dependent primordial tensor spectrum and, although small in magnitude, it dominates the primordial signal for some cosmological models. We confirm our analytical results by direct numerical integration of the equations of motion.

DOI: 10.1103/PhysRevD.76.084019 PACS numbers: 04.30.−w, 04.20.−q, 98.80.Jk

I. INTRODUCTION

Arguably the most striking prediction of inflationary cosmology [1] is the causal generation of nearly scale-invariant spectra of both scalar (energy density) and tensor (gravitational wave, GW) perturbations. The natural prediction is that the scalar and tensor amplitudes are comparable within 1 or 2 orders of magnitude of one another by virtue of the fact that both are created by the same de Sitter quantum process. The existence of a scalar spectrum is now firmly established by measurements of the cosmic microwave background (CMB) [2] and large-scale structure [3], and its amplitude is well determined. Tensor fluctuations, on the other hand, have yet to be detected, although current measurements have only begun to probe the expected range of amplitudes.

Detecting primordial tensor fluctuations is an important milestone because it rules out a whole class of alternative cosmological scenarios, like the ekpyrotic [4] and cyclic models [5], which produce virtually the identical scalar spectrum as inflation but a completely different tensor spectrum. In particular, the primordial tensor contribution in ekpyrotic/cyclic models is exponentially smaller and more blue [6]. Detection of a primordial tensor signal is therefore widely regarded as a smoking gun signature of inflation. However, failing to detect the tensor modes at the expected level does not necessarily rule out inflation. The inflationary tensor signal can be suppressed by extra fine-tuning of the inflationary model and/or the addition of extra fields (e.g. hybrid inflation [7]) so that the background equation of state of the Universe, instead of changing smoothly during the final stages of inflation, undergoes a sequence of jerks and gyrations [8]. A number of studies have discussed the limits to how far a search for the tensor spectrum can go based on detector sensitivity and foregrounds [9].

At second order in perturbation theory the observed scalar spectrum sources the generation of secondary tensor modes [10]. In this paper, we analyze the stochastic spectrum of second-order gravitational waves induced by the first-order scalar perturbations. Since the scalar spectrum is already measured, this contribution to the tensor spectrum must exist and must be the same for both inflationary and ekpyrotic models because their predictions for the scalar spectrum match. For inflation, this second-order contribution is generically negligible, orders of magnitude smaller than the first-order contribution except for models with extreme fine-tuning. For ekpyrotic and cyclic models, the scalar-induced, second-order contribution computed here is actually the dominant contribution on astrophysical and cosmological scales, because the first-order tensor spectrum is always exponentially small compared to the scalar spectrum. Hence, the calculation here supersedes previous predictions of the tensor spectrum for ekpyrotic and cyclic models [6]. Because the gravitational wave spectrum we compute here is purely a consequence of the *observed* scalar spectrum and general relativistic evolution, any mechanism that accounts for the observed spectrum of scalar fluctuations also generates the same secondary tensor spectrum, provided Einstein's equations hold. Hence, this second-order signal provides an absolute *lower limit* on tensors from the early Universe.

Our work builds on important earlier work by Mollerach, Harari, and Matarrese [11] and Ananda,

*dbaumann@princeton.edu
†steinh@princeton.edu
‡ktakahas@princeton.edu
§ichiki@resceu.s.u-tokyo.ac.jp

Clarkson, and Wands [12]. Mollerach *et al.* [11] computed the effect of second-order gravitational waves on large-scale CMB polarization. They found that the second-order tensors dominate over the first-order signal if the ratio of the tensor-to-scalar amplitude on the largest observable wavelengths is $r < 10^{-6}$. Then, more recently, Ananda, Clarkson, and Wands [12] numerically studied the present spectrum of gravitational waves on very small scales accessible to direct-detection experiments like the big bang observer (BBO). Typically, the signal is expected to be at the extreme limit of the predicted sensitivity of BBO. Here we compute the complete spectrum of scalar-induced gravitational waves on all scales and discuss how it evolves with time. We analytically determine a critical scale above which second-order gravitational waves do *not* redshift. This nontrivial transfer function for scalar-induced gravitational waves leads to an interesting feature in the current spectrum (see the schematic in Fig. 1) with a factor 10^7 enhancement of modes of order of the horizon size at matter-radiation equality relative to the scale-invariant small-scale spectrum. We confirm our analytical findings by numerical integration of the equations of motion.

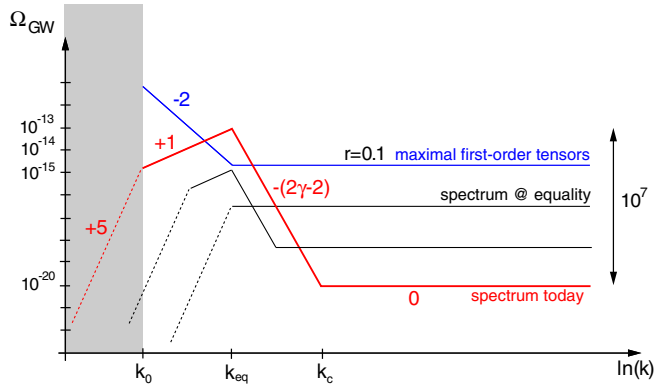

FIG. 1 (color online). *Spectra of first- and second-order gravitational waves:* This schematic illustrates the conjectured form of $\Omega_{GW}(k)$, the fraction of the critical density in gravitational waves per log-interval of wave number k, as derived in Sec. III. The topmost curve represents the typical first-order inflationary tensor spectrum. With fine-tuning, it can be suppressed below the level of the second-order, scalar-induced tensor perturbations (bottom curves). The bottom curves represent a sequence of times: matter-radiation equality (a_{eq}), redshift $z = 100$, and today (a_0). The scalar-induced tensor spectra shown here are for a perfectly scale-invariant scalar input spectrum ($n_s = 1$). If the scalar spectrum is blue ($n_s > 1$) the induced tensor spectrum is enhanced on small scales (large k), while a red spectrum ($n_s < 1$) suppresses tensor fluctuations on small scales (see Sec. V for cautionary remarks about extrapolating spectra to very small scales using the large-scale power law form of the scalar spectrum). Ω_{GW} is of course ill-defined on superhorizon scales. On superhorizon scales (dashed lines) we therefore formally define the rescaled tensor power spectrum, $k^2 P_h(k)$, but do *not* interpret it as an energy density of gravitational waves (see Sec. III).

The outline of the paper is as follows: In Sec. II, we derive the evolution equations for second-order tensor fluctuations sourced by first-order scalar fluctuations. Allowing for an anisotropic stress contribution to the energy-momentum tensor, we derive a general expression for the power spectrum of scalar-induced gravitational waves. This generalizes the work of Ref. [12]. In Sec. III, we analyze the spectrum using various approximations and scaling arguments. These analytical estimates are confirmed by direct numerical integration of the equations of motion in Sec. IV. Finally, we discuss the implications of these results in Sec. V. In two appendices we recall the Green's functions for gravitational waves and the transfer functions for first-order scalar fluctuations [13].

We use the following conventions: Throughout we employ natural units, $\hbar = c \equiv 1$, and (reduced) Planck mass $M_P^{-2} = 8\pi G \equiv \kappa^2$, as well as "East coast" signature for the metric, $(-, +, +, +)$. Greek indices, $\mu, \nu = 0, \ldots, 3$, denote four-dimensional spacetime indices, while roman indices, $i, j = 1, \ldots, 3$, are reserved for spatial indices. The parameter η is conformal time, $a(\eta)\mathrm{d}\eta = \mathrm{d}t$.

II. SECOND-ORDER TENSORS FROM FIRST-ORDER SCALARS

Let us recall some basic facts about second-order perturbation theory, before deriving the explicit form of the evolution equations for second-order, scalar-induced tensors. We consider perturbations to a flat Friedmann-Robertson-Walker (FRW) background, $g^{(0)}_{\mu\nu} = a^2(\eta)\eta_{\mu\nu}$,

$$g_{\mu\nu} = g^{(0)}_{\mu\nu} + \delta g_{\mu\nu}, \tag{1}$$

where $g^{(0)}_{\mu\nu}$ satisfies the 0th-order Einstein equations, $G^{(0)}_{\mu\nu} = \kappa^2 T^{(0)}_{\mu\nu}$,

$$\mathcal{H}^2 = \frac{\kappa^2 a^2}{3}\rho^{(0)}, \qquad \mathcal{H} \equiv \partial_\eta \ln a,$$
$$\mathcal{H}^2 - \mathcal{H}' = \frac{\kappa^2 a^2}{2}(\rho^{(0)} + P^{(0)}). \tag{2}$$

Here $\rho^{(0)}$ and $P^{(0)}$ are the homogeneous background density and pressure, respectively, and $(\ldots)'$ denotes a derivative with respect to conformal time, η. Including to linear order the small quantum perturbations to the metric and energy density, the solution to the first-order Einstein equations, $G^{(1)}_{\mu\nu} = \kappa^2 T^{(1)}_{\mu\nu}$, can be decomposed into independent scalar, vector, and tensor modes. At linear order, different k-modes in Fourier space are independent. This is in contrast to the second-order Einstein equations, $G^{(2)}_{\mu\nu} = \kappa^2 T^{(2)}_{\mu\nu}$, where different k-modes mix and scalar, vector, and tensor modes are not independent. However, it is important to notice that, at second order, there is no mixing between second-order scalar, vector, and tensor modes. On the other hand, there is a second-order contribution to the tensor mode, $h^{(2)}_{ij}$, that depends quadratically on the first-order

scalar metric perturbation. This contribution, the "scalar-induced" tensor mode, is the focus of this paper.[1]

A. Evolution equations

To compute the second-order, scalar-induced tensor mode we begin with the following perturbed metric

$$ds^2 = a^2(\eta)[-(1+2\Phi^{(1)}+2\Phi^{(2)})d\eta^2 + 2V_i^{(2)}d\eta dx^i + \{(1-2\Psi^{(1)}-2\Psi^{(2)})\delta_{ij} + \tfrac{1}{2}h_{ij}\}dx^i dx^j], \quad (3)$$

where $h_{ij} \equiv h_{ij}^{(2)}$ and we have ignored first-order vector and tensor perturbations. Here and in the following, the superscripts are formal labels for the order of the perturbation. The second-order Einstein tensor and energy-momentum tensor are [15]

$$G^{(2)i}{}_j = a^{-2}[\tfrac{1}{4}(h_j^{i\prime\prime} + 2\mathcal{H}h_j^{i\prime} - \nabla^2 h_j^i) + 2\Phi^{(1)}\partial^i\partial_j\Phi^{(1)} - 2\Psi^{(1)}\partial^i\partial_j\Phi^{(1)} + 4\Psi^{(1)}\partial^i\partial_j\Psi^{(1)} + \partial^i\Phi^{(1)}\partial_j\Phi^{(1)} - \partial^i\Phi^{(1)}\partial_j\Psi^{(1)} - \partial^i\Psi^{(1)}\partial_j\Phi^{(1)} + 3\partial^i\Psi^{(1)}\partial_j\Psi^{(1)} + (\Phi^{(2)}, \Psi^{(2)}, V_i^{(2)} \text{ terms}) + (\text{diagonal part})\delta_j^i], \quad (4)$$

and

$$T^{(2)i}{}_j = (\rho^{(0)} + P^{(0)})v^{(1)i}v_j^{(1)} + P^{(0)}\Pi^{(2)i}{}_j + P^{(1)}\Pi^{(1)i}{}_j + P^{(2)}\delta_j^i, \quad (5)$$

where ρ, P, v, and Π are energy density, pressure, velocity, and anisotropic stress, respectively. We act on the spatial components of the Einstein equations with the projection tensor $\hat{\mathcal{T}}_{ij}{}^{lm}$ [12],

$$\hat{\mathcal{T}}_{ij}{}^{lm}G_{lm}^{(2)} = \kappa^2\hat{\mathcal{T}}_{ij}{}^{lm}T_{lm}^{(2)}. \quad (6)$$

We will define the operator $\hat{\mathcal{T}}_{ij}{}^{lm}$ explicitly below, but we note here that it extracts the transverse, traceless part of any tensor and eliminates the terms involving $\Phi^{(2)}$, $\Psi^{(2)}$, $V_i^{(2)}$, $P^{(2)}$ and the scalar and vector parts of $\Pi^{(2)i}{}_j$ in the second-order Einstein equations. Using the following first-order relations,

$$P^{(1)} \equiv c_s^2\rho^{(1)}, \quad (7)$$

$$\rho^{(1)} = -\frac{2}{\kappa^2 a^2}[3\mathcal{H}(\mathcal{H}\Phi^{(1)} - \Psi^{(1)\prime}) + \nabla^2\Psi^{(1)}], \quad (8)$$

$$v_i^{(1)} = -\frac{2}{\kappa^2 a^2(\rho^{(0)}+P^{(0)})}\partial_i(\Psi^{(1)\prime} + \mathcal{H}\Phi^{(1)}), \quad (9)$$

$$\Pi^{(1)i}{}_j = -\frac{1}{\kappa^2 a^2 P^{(0)}}\left(\partial^i\partial_j - \frac{1}{3}\delta_j^i\nabla^2\right)(\Phi^{(1)} - \Psi^{(1)}), \quad (10)$$

[1]Scalar-induced vector modes were studied in [14].

the evolution equation (6) can be written as follows,

$$h_{ij}'' + 2\mathcal{H}h_{ij}' - \nabla^2 h_{ij} = -4\hat{\mathcal{T}}_{ij}{}^{lm}\mathcal{S}_{lm}, \quad (11)$$

where we have neglected the tensor part of $\Pi^{(2)i}{}_j$ and defined

$$\mathcal{S}_{ij} \equiv 2\Phi\partial^i\partial_j\Phi - 2\Psi\partial^i\partial_j\Phi + 4\Psi\partial^i\partial_j\Psi + \partial^i\Phi\partial_j\Phi - \partial^i\Phi\partial_j\Psi - \partial^i\Psi\partial_j\Phi + 3\partial^i\Psi\partial_j\Psi - \frac{4}{3(1+w)\mathcal{H}^2}\partial_i(\Psi' + \mathcal{H}\Phi)\partial_j(\Psi' + \mathcal{H}\Phi) - \frac{2c_s^2}{3w\mathcal{H}^2}[3\mathcal{H}(\mathcal{H}\Phi - \Psi') + \nabla^2\Psi]\partial_i\partial_j(\Phi - \Psi). \quad (12)$$

Here, $w \equiv P^{(0)}/\rho^{(0)}$, $\Phi \equiv \Phi^{(1)}$, and $\Psi \equiv \Psi^{(1)}$. We define the Fourier transform of tensor metric perturbations as

$$h_{ij}(\mathbf{x}, \eta) = \int \frac{d^3\mathbf{k}}{(2\pi)^{3/2}} e^{i\mathbf{k}\cdot\mathbf{x}}[h_{\mathbf{k}}(\eta)\mathsf{e}_{ij}(\mathbf{k}) + \bar{h}_{\mathbf{k}}(\eta)\bar{\mathsf{e}}_{ij}(\mathbf{k})], \quad (13)$$

where the two time-independent polarization tensors e_{ij} and $\bar{\mathsf{e}}_{ij}$ may be expressed in terms of orthonormal basis vectors $\mathbf{e}$ and $\bar{\mathbf{e}}$ orthogonal to $\mathbf{k}$,

$$\mathsf{e}_{ij}(\mathbf{k}) \equiv \tfrac{1}{\sqrt{2}}[\mathsf{e}_i(\mathbf{k})\mathsf{e}_j(\mathbf{k}) - \bar{\mathsf{e}}_i(\mathbf{k})\bar{\mathsf{e}}_j(\mathbf{k})], \quad (14)$$

$$\bar{\mathsf{e}}_{ij}(\mathbf{k}) \equiv \tfrac{1}{\sqrt{2}}[\mathsf{e}_i(\mathbf{k})\bar{\mathsf{e}}_j(\mathbf{k}) + \bar{\mathsf{e}}_i(\mathbf{k})\mathsf{e}_j(\mathbf{k})]. \quad (15)$$

In terms of these polarization tensors, the projection tensor in (6) and (11) is

$$\hat{\mathcal{T}}_{ij}{}^{lm}\mathcal{S}_{lm} = \int \frac{d^3\mathbf{k}}{(2\pi)^{3/2}} e^{i\mathbf{k}\cdot\mathbf{x}}[\mathsf{e}_{ij}(\mathbf{k})\mathsf{e}^{lm}(\mathbf{k}) + \bar{\mathsf{e}}_{ij}(\mathbf{k})\bar{\mathsf{e}}^{lm}(\mathbf{k})]\mathcal{S}_{lm}(\mathbf{k}), \quad (16)$$

where

$$\mathcal{S}_{lm}(\mathbf{k}) = \int \frac{d^3\mathbf{x}'}{(2\pi)^{3/2}} e^{-i\mathbf{k}\cdot\mathbf{x}'}\mathcal{S}_{lm}(\mathbf{x}'). \quad (17)$$

In Fourier space, the equation of motion for the gravitational wave amplitude h (for either polarization h or $\bar{h}$) becomes

$$h_{\mathbf{k}}'' + 2\mathcal{H}h_{\mathbf{k}}' + k^2 h_{\mathbf{k}} = \mathcal{S}(\mathbf{k}, \eta), \quad (18)$$

where the source term, $\mathcal{S}$, is a convolution of two first-order scalar perturbations at different wave numbers,

$$\mathcal{S}(\mathbf{k},\eta) = -4\mathsf{e}^{lm}(\mathbf{k})\mathcal{S}_{lm}(\mathbf{k})$$

$$= 4\int \frac{\mathrm{d}^3\tilde{\mathbf{k}}}{(2\pi)^{3/2}}\mathsf{e}^{lm}(\mathbf{k})\tilde{k}_l\tilde{k}_m\Bigg[\left\{\frac{7+3w}{3(1+w)}-\frac{2c_s^2}{w}\right\}\Phi_{\tilde{\mathbf{k}}}(\eta)\Phi_{\mathbf{k}-\tilde{\mathbf{k}}}(\eta)+\left(1-\frac{2c_s^2\tilde{k}^2}{3w\mathcal{H}^2}\right)\Psi_{\tilde{\mathbf{k}}}(\eta)\Psi_{\mathbf{k}-\tilde{\mathbf{k}}}(\eta)$$
$$+\frac{2c_s^2}{w}\left(1+\frac{\tilde{k}^2}{3\mathcal{H}^2}\right)\Phi_{\tilde{\mathbf{k}}}(\eta)\Psi_{\mathbf{k}-\tilde{\mathbf{k}}}(\eta)+\left\{\frac{8}{3(1+w)}+\frac{2c_s^2}{w}\right\}\frac{1}{\mathcal{H}}\Phi_{\tilde{\mathbf{k}}}(\eta)\Psi'_{\mathbf{k}-\tilde{\mathbf{k}}}(\eta)-\frac{2c_s^2}{w\mathcal{H}}\Psi_{\tilde{\mathbf{k}}}(\eta)\Psi'_{\mathbf{k}-\tilde{\mathbf{k}}}(\eta)$$
$$+\frac{4}{3(1+w)\mathcal{H}^2}\Psi'_{\tilde{\mathbf{k}}}(\eta)\Psi'_{\mathbf{k}-\tilde{\mathbf{k}}}(\eta)\Bigg]. \tag{19}$$

Equation (19) reduces to the expression in [12] in the limit $\Psi\to\Phi$, $w\to 1/3$, and $c_s^2\to 1/3$. The limit $\Psi\to\Phi$, $w\to 0$, and $c_s^2\to 0$ was discussed in [11].

B. Power spectrum

The power spectrum of tensor metric perturbations, $P_h(k,\eta)$, is defined as follows

$$\langle h_{\mathbf{k}}(\eta)h_{\mathbf{K}}(\eta)\rangle = \frac{2\pi^2}{k^3}\delta(\mathbf{k}+\mathbf{K})P_h(k,\eta). \tag{20}$$

We now derive an expression for the power spectrum of scalar-induced second-order gravitational waves by solving Eq. (18). It is convenient to remove the Hubble damping term in (18) by defining $ah_{\mathbf{k}}\equiv v_{\mathbf{k}}$, where $v_{\mathbf{k}}$ satisfies the following equation of motion

$$v''_{\mathbf{k}}+\left(k^2-\frac{a''}{a}\right)v_{\mathbf{k}} = a\mathcal{S}. \tag{21}$$

The particular solution of (18) is then found by the Green's function method

$$h_{\mathbf{k}}(\eta) = \frac{1}{a(\eta)}\int \mathrm{d}\tilde{\eta}\, g_{\mathbf{k}}(\eta;\tilde{\eta})[a(\tilde{\eta})\mathcal{S}(\mathbf{k},\tilde{\eta})], \tag{22}$$

where

$$g''_{\mathbf{k}}+\left(k^2-\frac{a''}{a}\right)g_{\mathbf{k}} = \delta(\eta-\tilde{\eta}). \tag{23}$$

Exact solutions to (23) for both matter and radiation domination are derived in Appendix A. Substituting the solution (22) into the expression for the tensor power spectrum (20) we find

$$\langle h_{\mathbf{k}}(\eta)h_{\mathbf{K}}(\eta)\rangle = \frac{1}{a^2(\eta)}\int_{\eta_0}^{\eta}\mathrm{d}\tilde{\eta}_2\int_{\eta_0}^{\eta}\mathrm{d}\tilde{\eta}_1 a(\tilde{\eta}_1)a(\tilde{\eta}_2)$$
$$\times g_{\mathbf{k}}(\eta;\tilde{\eta}_1)g_{\mathbf{K}}(\eta;\tilde{\eta}_2)\langle\mathcal{S}(\mathbf{k},\tilde{\eta}_1)\mathcal{S}(\mathbf{K},\tilde{\eta}_2)\rangle. \tag{24}$$

The source term (19) may be written in the following form

$$\mathcal{S}(\mathbf{k},\eta)\equiv\int \mathrm{d}^3\tilde{\mathbf{k}}\,\mathsf{e}(\mathbf{k},\tilde{\mathbf{k}})f(\mathbf{k},\tilde{\mathbf{k}},\eta)\psi_{\mathbf{k}-\tilde{\mathbf{k}}}\psi_{\tilde{\mathbf{k}}}, \tag{25}$$

where

$$\mathsf{e}(\mathbf{k},\tilde{\mathbf{k}})\equiv\mathsf{e}^{ij}(k)\tilde{k}_i\tilde{k}_j = \tilde{k}^2[1-\mu^2],\qquad \mu\equiv\frac{\mathbf{k}\cdot\tilde{\mathbf{k}}}{k\tilde{k}}, \tag{26}$$

and

$$f(\mathbf{k},\tilde{\mathbf{k}},\eta)\equiv 4\Bigg[\left\{\frac{7+3w}{3(1+w)}-\frac{2c_s^2}{w}\right\}\Phi(\tilde{k}\eta)\Phi(|\mathbf{k}-\tilde{\mathbf{k}}|\eta)+\left(1-\frac{2c_s^2\tilde{k}^2}{3w\mathcal{H}^2}\right)\Psi(\tilde{k}\eta)\Psi(|\mathbf{k}-\tilde{\mathbf{k}}|\eta)$$
$$+\frac{2c_s^2}{w}\left(1+\frac{\tilde{k}^2}{3\mathcal{H}^2}\right)\Phi(\tilde{k}\eta)\Psi(|\mathbf{k}-\tilde{\mathbf{k}}|\eta)+\left\{\frac{8}{3(1+w)}+\frac{2c_s^2}{w}\right\}\frac{1}{\mathcal{H}}\Phi(\tilde{k}\eta)\Psi'(|\mathbf{k}-\tilde{\mathbf{k}}|\eta)$$
$$-\frac{2c_s^2}{w\mathcal{H}}\Psi(\tilde{k}\eta)\Psi'(|\mathbf{k}-\tilde{\mathbf{k}}|\eta)+\frac{4}{3(1+w)\mathcal{H}^2}\Psi'(\tilde{k}\eta)\Psi'(|\mathbf{k}-\tilde{\mathbf{k}}|\eta)\Bigg]. \tag{27}$$

Here we have split the first-order quantities into transfer functions, $\Phi(k\eta)$, $\Psi(k\eta)$, and primordial fluctuations $\psi_{\mathbf{k}}$,

$$\Phi_{\mathbf{k}}(\eta)\equiv\Phi(k\eta)\psi_{\mathbf{k}},\qquad \Psi_{\mathbf{k}}(\eta)\equiv\Psi(k\eta)\psi_{\mathbf{k}}. \tag{28}$$

The primordial fluctuations are characterized by the power spectrum,

$$\langle\psi_{\mathbf{k}}\psi_{\tilde{\mathbf{k}}}\rangle = \frac{2\pi^2}{k^3}P(k)\delta(\mathbf{k}+\tilde{\mathbf{k}}). \tag{29}$$

Observationally, it is found that $P(k)$ is nearly scale invariant, so that the following parametrization is appropriate

$$P(k) = \frac{4}{9}\Delta^2_{\mathcal{R}}(k_0)\left(\frac{k}{k_0}\right)^{n_s-1}, \tag{30}$$

where recent CMB and large-scale structure results [2,3] imply $\Delta^2_{\mathcal{R}}(k_0=0.002\ \mathrm{Mpc}^{-1}) = (2.40\pm0.12)\times10^{-9}$ and $n_s(k_0)\sim 0.94$–1.10 (0.95 ± 0.02; no tensors). Finally, the correlator in Eq. (24) can be computed using Wick's

theorem

$$\langle \mathcal{S}(\mathbf{k}, \tilde{\eta}_1)\mathcal{S}(\mathbf{K}, \tilde{\eta}_2)\rangle = \int d^3\tilde{\mathbf{k}} e(\mathbf{k}, \tilde{\mathbf{k}}) f(\mathbf{k}, \tilde{\mathbf{k}}, \tilde{\eta}_1) \int d^3\tilde{\mathbf{K}} e(\mathbf{K}, \tilde{\mathbf{K}}) f(\mathbf{K}, \tilde{\mathbf{K}}, \tilde{\eta}_2) \langle \psi_{\mathbf{k}-\tilde{\mathbf{k}}}\psi_{\tilde{\mathbf{k}}}\psi_{\mathbf{K}-\tilde{\mathbf{K}}}\psi_{\tilde{\mathbf{K}}}\rangle$$
$$= \delta(\mathbf{k}+\mathbf{K}) \int d^3\tilde{\mathbf{k}} e(\mathbf{k}, \tilde{\mathbf{k}})^2 f(\mathbf{k}, \tilde{\mathbf{k}}, \tilde{\eta}_1)[f(\mathbf{k}, \tilde{\mathbf{k}}, \tilde{\eta}_2) + f(\mathbf{k}, \mathbf{k}-\tilde{\mathbf{k}}, \tilde{\eta}_2)] \frac{P(|\mathbf{k}-\tilde{\mathbf{k}}|)}{|\mathbf{k}-\tilde{\mathbf{k}}|^3} \frac{P(\tilde{k})}{\tilde{k}^3}, \quad (31)$$

and the power spectrum of scalar-induced second-order gravitational waves is

$$P_h(k, \eta) = \int_0^\infty d\tilde{k} \int_{-1}^1 d\mu P(|\mathbf{k}-\tilde{\mathbf{k}}|) P(\tilde{k}) \mathcal{F}(k, \tilde{k}, \mu; \eta), \quad (32)$$

where

$$\mathcal{F}(k, \tilde{k}, \mu; \eta) \equiv \frac{[1-\mu^2]^2}{a^2(\eta)} \frac{k^3\tilde{k}^3}{|\mathbf{k}-\tilde{\mathbf{k}}|^3} \int_{\eta_0}^{\eta} d\tilde{\eta}_2 d\tilde{\eta}_1 a(\tilde{\eta}_1) a(\tilde{\eta}_2) g_k(\eta; \tilde{\eta}_1) g_k(\eta; \tilde{\eta}_2) f(\mathbf{k}, \tilde{\mathbf{k}}, \tilde{\eta}_1)$$
$$\times [f(\mathbf{k}, \tilde{\mathbf{k}}, \tilde{\eta}_2) + f(\mathbf{k}, \mathbf{k}-\tilde{\mathbf{k}}, \tilde{\eta}_2)]. \quad (33)$$

Notice that the power spectrum $P_h(k, \eta)$ is defined completely in terms of the Green's function $g_{\mathbf{k}}$ (Appendix A), the transfer functions Φ and Ψ (Appendix B), and the primordial power spectrum of first-order scalar fluctuations, $P(k)$ (WMAP [2]).

III. ANALYTICAL DESCRIPTION OF THE SPECTRUM

In this section we estimate the complete spectrum of scalar-induced gravitational waves analytically. To simplify the analysis we neglect anisotropic stress and set $\Psi = \Phi$. In Sec. IV we evaluate the exact spectrum numerically including anisotropic stress and show that this gives only a small correction. With $\Psi = \Phi$, the source term of the equation of motion (18) can be expressed solely by the Bardeen potential Φ,

$$h_k'' + 2\mathcal{H}h_k' + k^2 h_k = \mathcal{S}(\Phi(k\eta)), \quad (34)$$

and $f(\mathbf{k}, \tilde{\mathbf{k}}, \eta)$ in Eq. (27) is expressed by a single transfer function Φ,

$$\frac{3(1+w)}{4} f(\mathbf{k}, \tilde{\mathbf{k}}, \eta) = 2(5+3w)\Phi(|\mathbf{k}-\tilde{\mathbf{k}}|\eta)\Phi(|\tilde{\mathbf{k}}|\eta)$$
$$+ 4(2\eta\Phi(|\mathbf{k}-\tilde{\mathbf{k}}|\eta)$$
$$+ \eta^2\Phi'(|\mathbf{k}-\tilde{\mathbf{k}}|\eta))\Phi'(|\tilde{\mathbf{k}}|\eta). \quad (35)$$

In Appendix B we show that the transfer function for first-order scalar modes can be written in the following form

$$\Phi(k\eta) = \begin{cases} \frac{1}{1+k^2\eta^2} & \eta < \eta_{\rm eq} \\ \frac{1}{1+k^2\eta_{\rm eq}^2} & \eta > \eta_{\rm eq} \end{cases}. \quad (36)$$

To study the generation of h induced by $\mathcal{S}$ we make the approximation that gravitational waves are produced instantaneously when the relevant mode enters the horizon. The subsequent evolution of the tensor mode is scale dependent and determined by the time evolution of the scalar source term (see Fig. 2). Scalar-induced gravitational waves redshift as long as their magnitude is greater than $\mathcal{S}/k^2$. After that they freeze at a constant value maintained by the constant source term during matter domination. We define the transfer function for scalar-induced gravitational waves, $t(k, \eta)$, as follows

$$h_k(\eta) \equiv t(k, \eta) h_k^{(\rm i)}, \quad (37)$$

where $h_k^{(\rm i)}$ is the value of h_k just after the instantaneous generation of gravitational waves after horizon entry (see Fig. 2). We estimate $h_k^{(\rm i)}$ by dropping time derivatives in the equation of motion (34) (since $k\eta > 1$ after horizon entry)

$$h_k^{(\rm i)} \sim \frac{1}{k^2}\mathcal{S}^{(\rm i)}. \quad (38)$$

In Sec. III A we calculate the initial power spectrum at the time of horizon crossing,

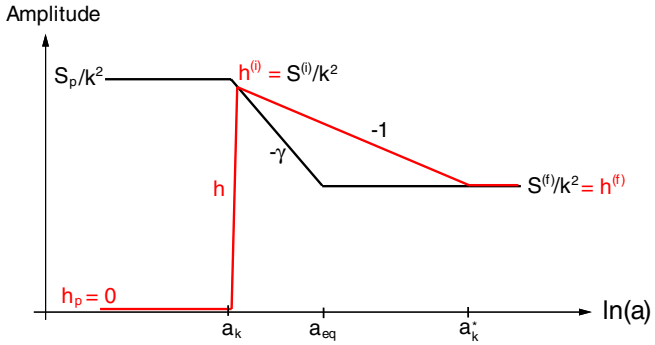

FIG. 2 (color online). *Evolution of scalar source and induced gravitational waves.* Second-order tensors, h, are generated when the mode k enters the horizon at a_k. If horizon entry occurs during the radiation dominated era, then the scalar source decays as $a^{-\gamma}$ until matter-radiation equality, $a_{\rm eq}$. During matter domination the scalar source terms remain at a constant value, $\mathcal{S}^{(\rm f)}$. Gravitational waves redshift like a^{-1} as long as $h > \mathcal{S}^{(\rm f)}/k^2$, but remain at a constant amplitude maintained by the constant source term after that, $a > a_k^*$.

$$P_h^{(\mathrm{i})}(k,\eta_\mathrm{i}(k)) \equiv \frac{k^3}{2\pi^2}\langle (h_k^{(\mathrm{i})})^2\rangle, \tag{39}$$

where $\eta_\mathrm{i}(k) \sim k^{-1}$ is the conformal time when a comoving scale k enters the horizon. This initial spectrum is processed using the tensor transfer function, $t(k,\eta)$, which we derive in Sec. III B. Finally, in Sec. III C, we put these results together and compute the relative energy density of scalar-induced gravitational waves

$$\begin{aligned}\Omega_{\mathrm{GW}}^{(2)}(k,\eta) &= \frac{1}{6\pi^2\mathcal{H}^2(\eta)}k^2t^2(k,\eta)P_h^{(\mathrm{i})}(k)\\ &= \frac{a(\eta)k^2}{a_{\mathrm{eq}}k_{\mathrm{eq}}^2}t^2(k,\eta)P_h^{(\mathrm{i})}(k).\end{aligned} \tag{40}$$

A. Power spectrum at horizon crossing

In this section we estimate the k-scaling of the horizon power spectrum of scalar-induced gravitational waves. The horizon amplitude $h_k^{(\mathrm{i})}$ is estimated from the equation of motion (34) as follows

$$\begin{aligned}h_k^{(\mathrm{i})} &\sim \frac{1}{k^2}\mathcal{S}^{(\mathrm{i})}\\ &\sim \frac{1}{k^2}\int \mathrm{d}^3\tilde{\mathbf{k}}\tilde{k}^2(1-\mu^2)\Phi(\tilde{k}\eta_\mathrm{i})\Phi(|\mathbf{k}-\tilde{\mathbf{k}}|\eta_\mathrm{i})\psi_{\tilde{\mathbf{k}}}\psi_{\mathbf{k}-\tilde{\mathbf{k}}},\end{aligned} \tag{41}$$

and its power spectrum is

$$\begin{aligned}\langle h_k^{(\mathrm{i})}h_K^{(\mathrm{i})}\rangle &\sim \frac{1}{k^2K^2}\int \mathrm{d}^3\tilde{\mathbf{k}}\mathrm{d}^3\tilde{\mathbf{K}}\tilde{k}^2\tilde{K}^2(1-\mu^2)(1-\tilde{\mu}^2)\Phi(\tilde{k}\eta_\mathrm{i})\Phi(|\mathbf{k}-\tilde{\mathbf{k}}|\eta_\mathrm{i})\Phi(\tilde{K}\eta_\mathrm{i})\Phi(|\mathbf{K}-\tilde{\mathbf{K}}|\eta_\mathrm{i})\langle\psi_{\tilde{\mathbf{k}}}\psi_{\mathbf{k}-\tilde{\mathbf{k}}}\psi_{\tilde{\mathbf{K}}}\psi_{\mathbf{K}-\tilde{\mathbf{K}}}\rangle\\ &\sim \frac{1}{k^4}\delta(\mathbf{k}+\mathbf{K})\int \mathrm{d}^3\tilde{\mathbf{k}}\tilde{k}^4(1-\mu^2)^2\Phi^2(\tilde{k}\eta_\mathrm{i})\Phi^2(|\mathbf{k}-\tilde{\mathbf{k}}|\eta_\mathrm{i})\frac{P(\tilde{k})}{\tilde{k}^3}\frac{P(|\mathbf{k}-\tilde{\mathbf{k}}|)}{|\mathbf{k}-\tilde{\mathbf{k}}|^3}.\end{aligned} \tag{42}$$

Hence,

$$P_h^{(\mathrm{i})}(k) \equiv \frac{k^3}{2\pi^2}\langle (h_k^{(\mathrm{i})})^2\rangle \sim \frac{1}{k}\int \mathrm{d}^3\tilde{\mathbf{k}}\tilde{k}^4(1-\mu^2)^2\Phi^2(\tilde{k}\eta_\mathrm{i})\Phi^2(|\mathbf{k}-\tilde{\mathbf{k}}|\eta_\mathrm{i})\frac{P(\tilde{k})}{\tilde{k}^3}\frac{P(|\mathbf{k}-\tilde{\mathbf{k}}|)}{|\mathbf{k}-\tilde{\mathbf{k}}|^3}. \tag{43}$$

To compute (43) we use the transfer function for the scalar potential (36) and assume a scale-invariant spectrum, $P(k) = \frac{4}{9}\Delta_{\mathcal{R}}^2$. (The scale-dependence of the scalar spectrum can be reinserted at the end of the computation). Here we have defined $\Delta_{\mathcal{R}}^2 \approx 10^{-9}$ as a measure of scalar power on COBE scales $k_0 \approx 0.002\ \mathrm{Mpc}^{-1}$. Hence, for the radiation dominated phase, we have

$$\begin{aligned}P_h^{(\mathrm{i})}(k,\eta_\mathrm{i}(k)) &\sim \frac{\Delta_{\mathcal{R}}^4}{k}\int_0^\infty \mathrm{d}\tilde{k}\int_{-1}^1 \mathrm{d}\mu(1-\mu^2)^2\frac{\tilde{k}^3}{(k^2+\tilde{k}^2-2k\tilde{k}\mu)^{3/2}}\frac{1}{[1+(\tilde{k}/k)^2]^2}\frac{1}{[1+(k^2+\tilde{k}^2-2k\tilde{k}\mu)/k^2]^2}\\ &= \Delta_{\mathcal{R}}^4\int_0^\infty \mathrm{d}x\int_{-1}^1 \mathrm{d}\mu(1-\mu^2)^2\frac{x^3}{(1+x^2-2x\mu)^{3/2}}\frac{1}{(1+x^2)^2}\frac{1}{(2+x^2-2x\mu)^2}\\ &\propto \Delta_{\mathcal{R}}^4,\end{aligned} \tag{44}$$

where we defined $x \equiv \tilde{k}/k$. On the other hand, for the matter dominated phase, we have

$$\begin{aligned}P_h^{(\mathrm{i})}(k,\eta_\mathrm{i}(k)) &\sim \frac{\Delta_{\mathcal{R}}^4}{k}\int_0^\infty \mathrm{d}\tilde{k}\int_{-1}^1 \mathrm{d}\mu(1-\mu^2)^2\frac{\tilde{k}^3}{(k^2+\tilde{k}^2-2k\tilde{k}\mu)^{3/2}}\frac{1}{[1+(\tilde{k}/k_{\mathrm{eq}})^2]^2}\frac{1}{[1+(k^2+\tilde{k}^2-2k\tilde{k}\mu)/k_{\mathrm{eq}}^2]^2}\\ &= \Delta_{\mathcal{R}}^4\int_0^\infty \mathrm{d}x\int_{-1}^1 \mathrm{d}\mu(1-\mu^2)^2\frac{x^3}{(1+x^2-2x\mu)^{3/2}}\frac{1}{(1+x^2y^2)^2}\frac{1}{[1+(1+x^2-2x\mu)y^2]^2},\end{aligned} \tag{45}$$

where $x \equiv \tilde{k}/k$ and $y \equiv k/k_{\mathrm{eq}} \ll 1$. Neglecting the μ-terms we find

$$\begin{aligned}P_h^{(\mathrm{i})}(k,\eta_\mathrm{i}(k)) &\sim \Delta_{\mathcal{R}}^4\int_0^\infty \mathrm{d}x\frac{x^3}{(1+x^2)^{3/2}}\frac{1}{(1+x^2y^2)^4} = \Delta_{\mathcal{R}}^4\left[\frac{5(1+6y^2)\arccos y}{16y(1-y^2)^{9/2}} - \frac{81+28y^2-4y^4}{48(1-y^2)^4}\right]\\ &\sim \frac{5\pi\Delta_{\mathcal{R}}^4}{32y} \propto \Delta_{\mathcal{R}}^4\frac{k_{\mathrm{eq}}}{k}.\end{aligned} \tag{46}$$

The power spectrum at horizon crossing therefore scales as follows

$$P_h^{(\mathrm{i})}(k) \propto \Delta_{\mathcal{R}}^4\begin{cases}\frac{k_{\mathrm{eq}}}{k} & k < k_{\mathrm{eq}}\\ 1 & k > k_{\mathrm{eq}}\end{cases}. \tag{47}$$

B. Second-order tensor transfer function

To compute the transfer function for second-order, scalar-induced gravitational waves we need to estimate the time evolution of the source term. In particular, the transfer function for modes that enter the horizon during radiation domination is sensitive only to the ratio of the source terms at horizon crossing, $\mathcal{S}^{(\mathrm{i})}$ and the asymptotic value after equality, $\mathcal{S}^{(\mathrm{f})}$ (see Fig. 2). We parametrize the decay of the source term during radiation domination as follows

$$\frac{\mathcal{S}^{(\mathrm{f})}}{\mathcal{S}^{(\mathrm{i})}} = \left(\frac{a_k}{a_{\mathrm{eq}}}\right)^{\gamma(k)}, \tag{48}$$

where we have allowed for a scale dependence of the effective decay rate. In the following we put limits on $\gamma(k)$ by considering the asymptotic evolution of subhorizon modes ($k\eta \gg 1$).

Let $x \equiv |\mathbf{k} - \tilde{\mathbf{k}}|\eta$ and $y \equiv |\tilde{\mathbf{k}}|\eta$. Using the following relations

$$\left(\frac{x(y,\mu)}{k\eta}\right)^2 = 1 + \left(\frac{y}{k\eta}\right)^2 - 2\left(\frac{y}{k\eta}\right)\mu \tag{49}$$

and

$$\psi_{\mathbf{k}-\tilde{\mathbf{k}}}\psi_{\tilde{\mathbf{k}}} \propto \frac{\eta^3}{x^{3/2}y^{3/2}}, \tag{50}$$

the source term may be written as follows

$$\mathcal{S}(\mathbf{k},\eta) \propto \frac{2\pi}{\eta^2}\int_0^\infty \mathrm{d}y \int_{-1}^{1} \mathrm{d}\mu[1-\mu^2]\frac{y^{5/2}}{x(y,\mu)^{3/2}} f(x,y), \tag{51}$$

where

$$2f(x,y) = \Phi(x)\Phi(y)[6 - y^2\Phi(x)\Phi(y)],$$

$$= \frac{1}{x^2+1}\frac{1}{y^2+1}\left[6 - \frac{1}{x^2+1}\frac{y^2}{y^2+1}\right]. \tag{52}$$

Let us estimate the integral (51). The limit $y \to 0$ is clearly suppressed by the phase space factor $y^{5/2}$ in the integrand. The limit $x \to 0$ ($y \to k\eta$, $\mu \to 1$) is suppressed by the projection factor $[1-\mu^2]$. To see this, first take the limit $y \to k\eta$,

$$\left(\frac{x}{k\eta}\right)^2 \to 2[1-\mu], \qquad \frac{1-\mu^2}{x^{3/2}} \to (1-\mu)^{1/4}(1+\mu). \tag{53}$$

This shows that the integrand vanishes in the limit $x \to 0$. In addition, large x and y are suppressed by the transfer function $f(x,y)$ (i.e. the decay of the Bardeen potential on subhorizon scales). The dominant contribution to the integral (51) therefore comes from regions of phase space where $\tilde{k} \sim k$ ($y \sim k\eta$) and $|\mathbf{k} - \tilde{\mathbf{k}}| \sim k$ ($x \sim k\eta$, $\mu \sim 0$). Let us therefore write

$$\mathcal{S} \propto \frac{1}{\eta^2}\int \mathrm{d}\ln y \int \mathrm{d}\ln(1-\mu)(1-\mu)^2(1+\mu)\frac{y^{7/2}}{x^{3/2}} \times \frac{1}{x^2+1}\frac{1}{y^2+1}\left[6 - \frac{1}{x^2+1}\frac{y^2}{y^2+1}\right] \tag{54}$$

and take the subhorizon limit $y, x \to k\eta > 1$, $\mu \to 0$

$$\mathcal{S} \propto \frac{1}{\eta^2}\frac{(k\eta)^{7/2}}{(k\eta)^{3/2}}\frac{1}{[(k\eta)^2+1]^2}\left[6 - \frac{(k\eta)^2}{[(k\eta)^2+1]^2}\right] \approx \frac{1}{\eta^2}\frac{1}{(k\eta)^2} \propto \frac{1}{a^4}. \tag{55}$$

Hence the source term decays at most as a^{-4} after the mode k enters the horizon during the radiation dominated era, i.e. $\gamma(k) < 4$. In fact, we expect the source term to decay considerably slower than that for a while after horizon crossing. The source will decay more and more quickly as the horizon grows much larger than the wavelength of the mode, finally reaching the asymptotic behavior that is proportional to a^{-4}. This leads us to expect that the effective γ in Eq. (48) will be significantly smaller than 4. Numerically, we find $\gamma \approx 3$ (see Sec. IV).

The transfer function for second-order gravitational waves is considerably different from the transfer function for first-order gravitational waves. First of all, modes which enter the horizon during matter domination have constant source terms and hence do *not* decay

$$t(k,\eta) = 1, \qquad k < k_{\mathrm{eq}}. \tag{56}$$

Next, consider the evolution of the scalar source term and induced gravitational waves for modes that enter the horizon during the radiation dominated era (see Fig. 2). Here, $k = a_k H$ defines the time of horizon entry (a_k) for a mode of wave number k. We assume that h grows very rapidly after horizon entry to become of order of the source term. Then $\mathcal{S}$ decays as $a^{-\gamma}$ (where our previous discussion implies $\gamma < 4$) while h redshifts as a^{-1} until h is equal to the final source term during matter domination at a_k^*. For $a > a_k^*$, h stays constant. We therefore have

$$\frac{h^{(\mathrm{f})}}{h^{(\mathrm{i})}} = \frac{a_k}{a_k^*} \approx \frac{\mathcal{S}^{(\mathrm{f})}}{\mathcal{S}^{(\mathrm{i})}} = \left(\frac{a_k}{a_{\mathrm{eq}}}\right)^{\gamma}, \tag{57}$$

and find

$$\frac{a_k}{a_k^*} = \left(\frac{a_k}{a_{\mathrm{eq}}}\right)^{\gamma} = \left(\frac{k}{k_{\mathrm{eq}}}\right)^{-\gamma}. \tag{58}$$

For a fixed time η, subhorizon modes with sufficiently large k have never settled down. The critical wave number at a time η can be obtained by substituting $a_k^* = a(\eta)$ into Eq. (58),

$$k_c(\eta) = \left(\frac{a(\eta)}{a_{\mathrm{eq}}}\right)^{1/(\gamma-1)} k_{\mathrm{eq}}. \tag{59}$$

Modes with $k > k_c(\eta)$ simply redshift like a^{-1},

$$t(k,\eta) = \frac{a_k}{a(\eta)} = \frac{a_{\rm eq}}{a(\eta)}\frac{1}{k\eta_{\rm eq}}, \qquad k > k_c(\eta). \tag{60}$$

The transfer function for second-order gravitational waves therefore takes the following interesting form

$$t(k,\eta) = \begin{cases} 1 & k < k_{\rm eq} \\ (\frac{k}{k_{\rm eq}})^{-\gamma} & k_{\rm eq} < k < k_c(\eta) \\ \frac{a_{\rm eq}}{a(\eta)}\frac{k_{\rm eq}}{k} & k > k_c(\eta) \end{cases}. \tag{61}$$

C. Spectrum of scalar-induced gravitational waves

Substituting the power spectrum at horizon crossing (47) and the tensor transfer function (61) into Eq. (40) for the relative spectral energy density of gravitational waves at time η, we find

$$\Omega^{(2)}_{\rm GW}(k,\eta) = A^{(2)}_{\rm GW}\Delta^4_{\mathcal{R}}(k_0)\left(\frac{k}{k_0}\right)^{2(n_s-1)} \begin{cases} \frac{a(\eta)}{a_{\rm eq}}\frac{k}{k_{\rm eq}} & k < k_{\rm eq} \\ \frac{a(\eta)}{a_{\rm eq}}(\frac{k}{k_{\rm eq}})^{-(2\gamma-2)} & k_{\rm eq} < k < k_c(\eta), \\ \frac{a_{\rm eq}}{a(\eta)} & k > k_c(\eta) \end{cases} \tag{62}$$

where an overall normalization constant $A^{(2)}_{\rm GW}$ has not been fixed by our analytical arguments. In Sec. IV we find $A^{(2)}_{\rm GW} \approx 10$ and $\gamma \approx 3$ (this is consistent with the normalization of the small-scale spectrum in [12]). Figure 1 summarizes this conjectured form of the scalar-induced gravitational wave spectrum. If the scalar spectrum can be treated by a power law with constant spectral index over a large range of scales, then a blue scalar spectrum ($n_s > 1$) enhances the tensor spectrum on small scales, while a red spectrum ($n_s < 1$) suppresses secondary tensor fluctuations. For comparison, the first-order spectrum of primordial gravitational waves in inflationary models can be expressed as

$$\Omega^{(1)}_{\rm GW}(k,\eta) = A^{(1)}_{\rm GW} r_0 \Delta^2_{\mathcal{R}}(k_0)\left(\frac{k}{k_0}\right)^{n_t} \times \begin{cases} \frac{a_{\rm eq}}{a(\eta)}(\frac{k}{k_{\rm eq}})^{-2} & k < k_{\rm eq} \\ \frac{a_{\rm eq}}{a(\eta)} & k > k_{\rm eq} \end{cases}, \tag{63}$$

where $A^{(1)}_{\rm GW} = 4.2 \times 10^{-2}$ and $r_0 \equiv \frac{P_h(k_0)}{P(k_0)}$ is the first-order tensor-to-scalar ratio evaluated on the scale of today's horizon, $k = k_0 \approx 0.002$ Mpc^{-1}. For single-field inflation, the spectral index of the primordial tensor spectrum, n_t, is related to the tensor-to-scalar ratio by the slow-roll consistency relation, $n_t = -r_0/8$. Matter-radiation equality is normalized by recent observations [2] $a_{\rm eq} \approx a_0/3400$.

The current tensor spectrum ($\eta = \eta_0$) on large scales ($k = k_{\rm eq}$) and on very small scales ($k \gg k_{\rm eq}$) (assuming inflation and $n_t \approx 0$ and $n_s \approx 1$) satisfies

$$\frac{\Omega^{(1)}_{\rm GW}(k = k_{\rm eq})}{\Omega^{(2)}_{\rm GW}(k = k_{\rm eq})} \approx r_0 \frac{A^{(1)}_{\rm GW}}{A^{(2)}_{\rm GW}}\frac{(\frac{a_{\rm eq}}{a_0})^2}{\Delta^2_{\mathcal{R}}(k_0)} \sim \frac{1}{10} r_0 \tag{64}$$

and

$$\frac{\Omega^{(1)}_{\rm GW}(k \gg k_{\rm eq})}{\Omega^{(2)}_{\rm GW}(k \gg k_{\rm eq})} \approx r_0 \frac{A^{(1)}_{\rm GW}}{A^{(2)}_{\rm GW}}\frac{1}{\Delta^2_{\mathcal{R}}(k_0)} \sim 10^6 r_0. \tag{65}$$

Hence, for inflation, on large scales the second-order, scalar-induced contribution *today*, in fact, dominates over the first-order contribution. This reflects the fact that second-order gravitational waves do *not* redshift on large scales, while first-order gravitational waves redshift on all scales. On small scales the first-order contribution dominates unless $r_0 < 10^{-6}$. For ekpyrotic/cyclic models, the first-order contribution (due to direct quantum fluctuations of the metric) is suppressed at $k = k_0$ by 60 orders of magnitude compared to the inflationary signal [6] and the spectrum is blue. Hence, in these models, the scalar-induced tensor modes, $\Omega^{(2)}_{\rm GW}$, comprise the dominant contribution on all scales.

CMB observations probe the time of photon-baryon decoupling at $a_{\rm CMB} \approx 3a_{\rm eq}$ and scales with $k < k_{\rm CMB} = (\frac{a_{\rm eq}}{a_{\rm CMB}})^{1/2} k_{\rm eq}$. The gravitational wave spectrum at that time satisfies

$$\frac{\Omega^{(1)}_{\rm GW}(k = k_{\rm CMB})}{\Omega^{(2)}_{\rm GW}(k = k_{\rm CMB})} \approx r_0 \frac{A^{(1)}_{\rm GW}}{A^{(2)}_{\rm GW}}\frac{(\frac{a_{\rm eq}}{a_{\rm CMB}})^2}{\Delta^2_{\mathcal{R}}(k_0)}\left(\frac{k_{\rm eq}}{k_{\rm CMB}}\right)^3 \sim 10^6 r_0 \tag{66}$$

and

$$\frac{\Omega^{(1)}_{\rm GW}(k \gg k_{\rm eq})}{\Omega^{(2)}_{\rm GW}(k \gg k_{\rm eq})} \approx r_0 \frac{A^{(1)}_{\rm GW}}{A^{(2)}_{\rm GW}}\frac{1}{\Delta^2_{\mathcal{R}}(k_0)} \sim 10^6 r_0. \tag{67}$$

Hence, at decoupling the first-order tensor signal dominates over the second-order, scalar-induced signal if $r_0 > 10^{-6}$. (This is consistent with the result of Mollerach *et al.* [11] who claim that second-order gravitational waves only have a significant imprint on the CMB if $r_0 < 10^{-8}$. This corresponds to second-order gravitational waves dominating over first-order gravitational waves at the time of recombination. Second-order effects can become visible for larger $r_0 < 10^{-6}$ if late time polarization generated by reionization is considered [11].)

For completeness, let us consider the power spectrum on superhorizon scales, e.g. during the matter dominated phase. On superhorizon scales, $k \ll \mathcal{H}$, the initial amplitude can be estimated from the equation of motion (34) by ignoring the gradient term and approximating the time derivatives by a factor of $\mathcal{H}$,

$$\mathcal{H}^2 h^{(\mathrm{i})}_{k\ll\mathcal{H}} \sim \mathcal{S}, \tag{68}$$

while $k^2 h^{(\mathrm{i})}_k \sim \mathcal{S}$ estimates the initial amplitude on the horizon scale. Hence, the initial power spectrum, $P^{(\mathrm{i})}_h$, on superhorizon scales is simply $(k/\mathcal{H})^4$ times the spectrum on the horizon scale

$$P^{(\mathrm{i})}_h(k) \propto \left(\frac{k}{\mathcal{H}}\right)^4 \times \Delta^4_{\mathcal{R}}(k_0)\frac{k_{\mathrm{eq}}}{k} \propto k^3, \qquad k < k_{\mathrm{hor}} \leq k_{\mathrm{eq}}. \tag{69}$$

Although the tensor power spectrum, P_h, is a well-defined gauge-invariant object on superhorizon scales, $\Omega^{(2)}_{\mathrm{GW}}$ is *not*. In particular, Eq. (40) is only defined on subhorizon scales. Nevertheless, we formally *define* $\Omega^{(2)}_{\mathrm{GW}} \propto k^2 P^{(\mathrm{i})}_h \propto k^5$ on superhorizon scales, but do *not* attribute physical meaning to it. This definition is useful, since all our results are presented in terms of $\Omega^{(2)}_{\mathrm{GW}}$ and the shape of the superhorizon spectrum gives a simple consistency check for the numerical analysis.

IV. NUMERICAL RESULTS FOR THE EXACT SPECTRUM

The spectrum of scalar-induced gravitational waves that we derived in Sec. II and discussed analytically in Sec. III can be evaluated exactly using standard numerical methods. The time evolution of the first-order perturbation variables necessary to compute the spectrum, $\Phi(k\eta)$ and $\Psi(k\eta)$, is obtained from publicly available Einstein-Boltzmann codes such as CMBFAST [16] or CAMB [17]. We first store the time evolution of Φ and Ψ in k-space, then convolve them according to Eq. (31). In practice, the range of k is taken to be $[10^{-5}\ \mathrm{Mpc}^{-1}, 500\ \mathrm{Mpc}^{-1}]$ and variables are evaluated at 50 uniformly spaced points per log-interval of k. We have checked that our results are stable under variations of the k-space boundaries and the discretization.

In the numerical analysis it is possible to incorporate the difference between Φ and Ψ resulting from anisotropic stress of the fluid because the Boltzmann equations of photons and neutrinos are solved explicitly in the code by expanding their distribution functions into multipole moments. (Neglecting anisotropic stress from neutrinos implies $\sim$10% errors for both first-order scalar and tensor perturbations [18,19]; see Fig. 5 in Appendix B. For second-order tensors we find that the inclusion of anisotropic stress typically has less than 1% effect on the amplitude of the spectrum.) Finally, we should mention here that our definition of c_s^2, Eq. (7), relates first-order pressure and energy density perturbations in the total matter, $P^{(1)}$ and $\rho^{(1)}$, including entropy perturbations, and thus it is scale dependent. We have derived and incorporated this numerically.

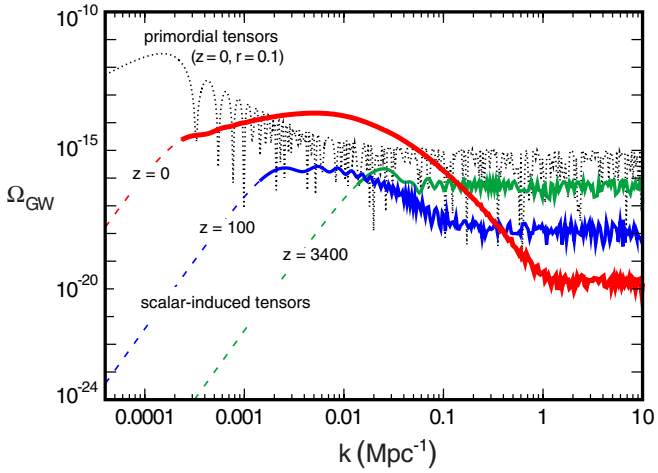

FIG. 3 (color online). Numerical spectra of scalar-induced gravitational waves (lower curves) and the scale-invariant primordial tensor spectrum for an inflationary model with tensor-to-scalar ratio $r = 0.1$ (upper curve). The scalar-induced spectra are shown at three different epochs, $z + 1 = 3400$, 100, and 1. Each curve has been extended, for pedagogical reasons, to modes with small wave numbers k that lie outside the horizon at the given epoch (dotted range of the three lower curves). Note that current $(z + 1 = 1)$ scalar-induced contributions cross the primordial inflationary contribution at intermediate wavelengths, as suggested by the schematic in Fig. 1. The simulation assumes a flat ΛCDM cosmology with the following model parameters: $\Delta^2_{\mathcal{R}}(k_0 = 0.002\ \mathrm{Mpc}^{-1}) = 2.4 \times 10^{-9}$, $n_s = 1$, $n_t = 0$, $r = 0.1$, $\Omega_b h^2 = 0.022$, $\Omega_m h^2 = 0.11$, $h = 0.7$.

The numerically calculated spectra are shown in Fig. 3. The shape of the scalar-induced gravitational wave spectrum agrees well with the analytical results of the previous section and the schematic diagram in Fig. 1, except for the fine-scale oscillations and the modest smoothing of the enhanced feature at large wavelengths. The scalar-induced spectrum is derived directly from observations of the scalar perturbations plus general relativity and is, in this sense, independent of the cosmological model for generating the primordial perturbations, e.g., inflation vs ekpyrotic/cyclic. However, the transfer function does depend weakly on the expansion rate and composition of the Universe, and, hence, the cosmological background parameters must be measured or otherwise specified.

V. DISCUSSION

Precise cosmological observations [2,3] have confirmed the existence of a nearly scale-invariant spectrum of pri-

mordial scalar fluctuations. These scalar fluctuations induce a second-order contribution to the spectrum of tensor perturbations that must be present for any cosmological model that accounts for the observed scalar spectrum. In particular, the computation of the second-order gravitational wave signal does *not* assume that the primordial perturbation spectra were generated by inflation—it only relies on the observed spectrum of scalar perturbations and general relativity.

In this paper we have computed the scalar-induced spectrum of gravitational waves produced in the early Universe and used the Einstein equations to evolve it to the present. We have extended previous approaches to this problem [11,12] by considering the complete cosmic history for the evolution of scalar-induced gravitational waves and allowing for anisotropic stress in our numerical work.

Perhaps the most interesting theoretical feature is that second-order gravitational waves do *not* redshift on large and intermediate scales, but are maintained at a constant amplitude by the scalar source terms. This leads to a transfer function for the scalar-induced gravitational waves that produces a (nearly) scale-invariant spectrum on small scales and interesting scale dependence on large and intermediate scales. In particular, there is a peak in the current spectrum of scalar-induced gravitational waves at the scale of the comoving horizon at matter-radiation equality (see Figs. 1, 3, and 4) that is likely to exceed the primordial tensor spectrum at the present epoch. Unfortunately, there are no known methods for directly probing the present gravitational wave spectrum on these scales (corresponding to the size of superclusters today). At earlier times, such as recombination, the feature was much smaller and so it only has small effects, e.g. on the CMB [11]. Hence, this substantial feature is likely to remain of purely academic interest in the foreseeable future.

On much smaller scales, which may be accessible to space-based laser-interferometer experiments (for a nice discussion see Ref. [20]), there are no measurements of the scalar perturbation spectrum, so one must rely on extrapolating from what is known about scalar perturbations on large scales, e.g. from measurements of the CMB and large-scale structure. Since these two wavelength regimes are separated by 16 orders of magnitude, extrapolation uncertainties can have important effects. For example, the dashed line in Fig. 4, which illustrates the extrapolation of the tensor spectrum based on a perfectly scale-invariant ($n_s = 1$) scalar spectrum, is an estimate of the induced small-scale tensor signal. Assuming that a nearly constant spectral index is a valid approximation from CMB scales to the smallest scales, a blue spectrum ($n_s > 1$) enhances scalar-induced tensor modes on small scales where direct gravitational wave detection experiments are planned, while a red spectrum ($n_s < 1$) suppresses them. Alternatively, for explicit inflationary models the whole spectrum can be computed directly from the inflaton potential $V(\phi)$ without expanding with respect to the CMB scale.[2] This allows a more reliable prediction of the level of gravitational waves on small scales.

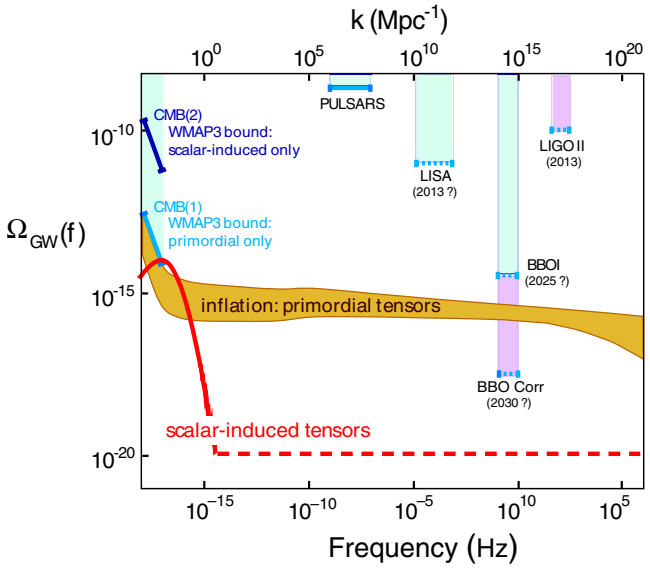

FIG. 4 (color online). *Observational prospects.* Shown are the theoretical predictions for the spectrum of scalar-induced versus primordial inflationary gravitational waves as predicted for the present epoch, along with the current (solid bars) and future (dashed bars) experimental bounds (figure modified from [8]). The band marked "primordial tensors" represents the inflationary predictions for minimally tuned models, as classified in [8]; with further fine-tuning, this spectrum can be shifted downwards. In contrast, the amplitude of the scalar-induced tensors is fixed by the observed amplitude of scalar fluctuations and therefore provides an absolute lower limit on the stochastic gravitational wave background. The CMB constraints depend on assumptions about the transfer function for gravitational waves to extrapolate constraints obtained at decoupling to the current spectrum. Since scalar-induced gravitational waves do not redshift on CMB scales, the CMB observations imply separate constraints on the current primordial and scalar-induced spectra. These constraints are labeled CMB(1) and CMB(2), respectively. The dashed section of the scalar-induced tensor spectrum illustrates extrapolation from CMB to direct-detection scales using a scale-invariant scalar spectrum ($n_s = 1$). Important uncertainties in the extrapolation between CMB and BBO scales are discussed in the main text.

Finally, let us consider the possible scenarios for future observations of the first- and second-order tensor signals and what they would signify:

(i) If a spectrum of gravitational waves is observed that conforms to a nearly scale-invariant, first-order tensor signal and with $r > 10^{-2}$ (as shown in Fig. 4), this would be a spectacular confirmation of the inflationary model of the Universe and completely rule

[2]For the first-order inflationary tensor spectrum this approach was followed by [21].

out ekpyrotic/cyclic models. The observation of such a signal with $r < 10^{-2}$ would also rule out ekpyrotic/cyclic models but, in addition, the inflationary scenario would be limited to models with extraordinary fine-tuning and/or extra fields and parameters [8].[3]

(ii) If no nearly scale-invariant, first-order tensor spectrum is detected but the scalar-induced, second-order tensor spectrum is observed (either by extremely sensitive CMB polarization experiments or small-scale direct-detection interferometers like BBO), then inflation could only be compatible with extreme enough fine-tuning to suppress the first-order contribution to the tensor signal, and alternatives like the ekpyrotic/cyclic models would be favored.

(iii) If future experiments show that there is no tensor signal at or above the level of the predicted scalar-induced tensor spectrum, either general relativity or the interpretation of the scalar fluctuations would have to be amiss.

In practice, observing the scalar-induced tensor signal is a long way off, at best, and perhaps even impossible given our current understanding of astrophysical foregrounds and detector limitations for both CMB and direct-detection experiments [9,24]. Nevertheless, we consider it interesting that the *observed* level of scalar fluctuations implies a model-independent *lower limit* on gravitational waves from the early Universe whose detailed features can be computed from a general relativistic description of cosmic evolution.

ACKNOWLEDGMENTS

It is a pleasure to thank Latham Boyle for a very careful reading of a draft of this paper. P. J. S. and D. B. thank Jo Dunkley and David Spergel for initial discussions that helped inspire this work. K. I. thanks Kouji Nakamura for useful discussions on second-order perturbations. K. I. and K. T. acknowledge the support by a Grant-in-Aid for the Japan Society for the Promotion of Science. P. J. S. and D. B. are supported by the U.S. Department of Energy Grant No. DE-FG02-91ER40671.

[3]In multifield models of inflation there is the hope that this fine-tuning (e.g. the tuning of mass ratios) may have a physical motivation. In addition, in inflationary models where the curvature perturbation is generated by a second field that is not the inflaton, like in the curvaton models [22], the first-order tensor signal is predicted to be unobservable. The second-order, scalar-induced tensor signal for the curvaton scenario was recently computed in [23]. In this case, the tensor signal induced by the isocurvature mode between the end of inflation and the curvaton decay always dominates over the tensor signal computed in this paper, i.e. the tensor signal created by second-order curvature perturbations after the curvaton decay.

APPENDIX A: GREEN'S FUNCTION FOR GRAVITATIONAL WAVES

In this section we derive exact Green's functions of Eq. (18) for both the radiation and matter dominated eras. The Green's function of a general second-order differential equation, $\hat{\mathcal{L}}g = \delta(\eta - \tilde{\eta})$ is defined as follows

$$g(\eta;\tilde{\eta}) \equiv \frac{v_1(\eta)v_2(\tilde{\eta}) - v_1(\tilde{\eta})v_2(\eta)}{v_1'(\tilde{\eta})v_2(\tilde{\eta}) - v_1(\tilde{\eta})v_2'(\tilde{\eta})}, \tag{A1}$$

in terms of the two homogeneous solutions v_1 and v_2, which satisfy $\hat{\mathcal{L}}v_i = 0$, for a general differential operator $\hat{\mathcal{L}}$. During the radiation dominated era the Green's function for the gravitational wave problem (23) reduces to

$$g_k'' + k^2 g_k = \delta(\eta - \tilde{\eta}), \tag{A2}$$

which has the following homogeneous solutions

$$v_1 = \sin(k\eta), \qquad v_2 = \cos(k\eta). \tag{A3}$$

Hence, the Green's function during the radiation dominated era ($\eta < \eta_{\rm eq}$) is

$$g_k(\eta;\tilde{\eta}) = \frac{1}{k}[\sin(k\eta)\cos(k\tilde{\eta}) - \sin(k\tilde{\eta})\cos(k\eta)]. \tag{A4}$$

During matter domination Eq. (23) reduces to

$$g_k'' + \left(k^2 - \frac{2}{\eta^2}\right)g_k = \delta(\eta - \tilde{\eta}), \tag{A5}$$

which has the following homogeneous solutions

$$v_1 = \eta j_1(x), \qquad v_2 = \eta y_1(x), \qquad x \equiv k\eta, \tag{A6}$$

where $j_1(x)$ and $y_1(x)$ are spherical Bessel functions. The Green's function during the matter dominated era ($\eta > \eta_{\rm eq}$) therefore is

$$g_k(\eta;\tilde{\eta}) = -\frac{x\tilde{x}}{k}[j_1(x)y_1(\tilde{x}) - j_1(\tilde{x})y_1(x)]. \tag{A7}$$

APPENDIX B: TRANSFER FUNCTION FOR FIRST-ORDER SCALAR MODES

The first-order scalar perturbations Φ and Ψ in Eq. (3) satisfy the following constraint equation [13]

$$k^2(\Phi - \Psi) = -4\kappa^2 a^2[\rho_\gamma \Theta_2 + \rho_\nu \mathcal{N}_2], \tag{B1}$$

where Θ_2 and $\mathcal{N}_2$ characterize the quadrupole moments of the photon (γ) and neutrino (ν) anisotropies, respectively. Θ_2 and $\mathcal{N}_2$ are determined by the solution to the Einstein-Boltzmann equations. In practice, these are solved numerically using CMBFAST [16] or CAMB [17] (see Fig. 5).

Since Θ_2 and $\mathcal{N}_2$ are typically negligibly small, analytical studies often assume $\Phi \approx \Psi$. In this case, the first-order equation of motion for the Bardeen potential is (e.g. [13])

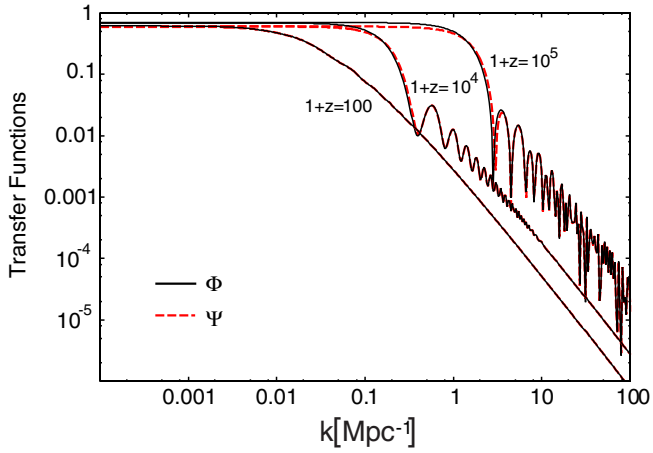

FIG. 5 (color online). *Transfer functions for* Φ *and* Ψ. Neutrino anisotropic stress leads to $\mathcal{O}(10)\%$ difference between Φ and Ψ [18].

$$\Phi'' + 3(1 + c_s^2)\mathcal{H}\Phi' - c_s^2\Delta\Phi + (2\mathcal{H}' + (1 + 3c_s^2)\mathcal{H}^2) \propto \delta S, \tag{B2}$$

where the right-hand side (RHS) is nonzero only in the presence of entropy perturbations, δS. For $p = w\rho$ and in the absence of entropy perturbations (i.e. $\delta S = 0$) this becomes

$$\Phi_{\mathbf{k}}'' + \frac{6(1 + w)}{1 + 3w}\frac{1}{\eta}\Phi_{\mathbf{k}}' + wk^2\Phi_{\mathbf{k}} = 0. \tag{B3}$$

Equation (B3) has the following exact solution

$$\Phi_{\mathbf{k}}(\eta) = y^{-\alpha}[C_1(k)J_\alpha(y) + C_2(k)Y_\alpha(y)], \qquad y \equiv \sqrt{w}k\eta, \qquad \alpha \equiv \frac{1}{2}\left(\frac{5 + 3w}{1 + 3w}\right), \tag{B4}$$

where J_α and Y_α are Bessel functions of order α. During the matter dominated era ($w = 0$) this becomes

$$\Phi_{\mathbf{k}}(\eta) = C_1(k) + \frac{C_2(k)}{y^5}, \tag{B5}$$

whereas during the radiation dominated era ($w = \frac{1}{3}$) we find

$$\Phi_{\mathbf{k}}(\eta) = \frac{1}{y^2}\left[C_1(k)\left(\frac{\sin y}{y} - \cos y\right) + C_2(k)\left(\frac{\cos y}{y} + \sin y\right)\right]. \tag{B6}$$

At early times $y = \sqrt{w}k\eta \ll 1$ this becomes asymptotically the primordial value,

$$\lim_{y\to 0}\Phi_{\mathbf{k}}(\eta) = C_1(k) = \psi_{\mathbf{k}}, \tag{B7}$$

where we have dropped the decaying mode ($C_2 \equiv 0$). For the growing mode solution we therefore obtain the following transfer function

$$\Phi(k\eta) = \begin{cases} \frac{1}{(k\eta)^2}\left(\frac{\sin[k\eta]}{k\eta} - \cos[k\eta]\right) & \eta < \eta_{\rm eq} \\ \text{const} & \eta > \eta_{\rm eq} \end{cases}. \tag{B8}$$

From this we see that superhorizon modes ($k\eta \ll 1$) freeze during the radiation era

$$\Phi(k\eta) = 1 + \mathcal{O}((k\eta)^2), \qquad k\eta \ll 1, \qquad \eta < \eta_{\rm eq}, \tag{B9}$$

while subhorizon modes ($k\eta > 1$) oscillate and decay as a^{-2}

$$\Phi(k\eta) = -\frac{\cos[k\eta]}{(k\eta)^2} = -\left(\frac{\eta_k}{\eta}\right)^2\cos[k\eta] = -\left(\frac{a_k}{a}\right)^2\cos[k\eta], \qquad k\eta > 1, \qquad \eta < \eta_{\rm eq}. \tag{B10}$$

Ignoring oscillations we therefore may write the following expression valid for both superhorizon and subhorizon modes

$$\Phi(k\eta) = \frac{1}{1 + (k\eta)^2}, \qquad \eta < \eta_{\rm eq}. \tag{B11}$$

The Bardeen potential freezes on all scales during matter domination.

[1] A. H. Guth, Phys. Rev. D **23**, 347 (1981); A. D. Linde, Phys. Lett. B **108**, 389 (1982); A. Albrecht and P. J. Steinhardt, Phys. Rev. Lett. **48**, 1220 (1982).

[2] D. N. Spergel *et al.* (WMAP Collaboration), Astrophys. J. Suppl. Ser. **148**, 175 (2003); H. V. Peiris *et al.*, Astrophys. J. Suppl. Ser. **148**, 213 (2003); D. N. Spergel *et al.*, Astrophys. J. Suppl. Ser. **170**, 377 (2007).

[3] M. Tegmark *et al.*, Phys. Rev. D **74**, 123507 (2006).

[4] J. Khoury, B. A. Ovrut, P. J. Steinhardt, and N. Turok, Phys. Rev. D **64**, 123522 (2001).

[5] P. J. Steinhardt and N. Turok, Science **296**, 1436 (2002); Phys. Rev. D **65**, 126003 (2002).

[6] L. A. Boyle, P. J. Steinhardt, and N. Turok, Phys. Rev. D **69**, 127302 (2004).

[7] A. D. Linde, Phys. Rev. D **49**, 748 (1994).

[8] L. A. Boyle, P. J. Steinhardt, and N. Turok, Phys. Rev. Lett. **96**, 111301 (2006).

[9] J. Bock *et al.*, arXiv:astro-ph/0604101.

[10] S. Matarrese, O. Pantano, and D. Saez, Phys. Rev. D **47**, 1311 (1993); Phys. Rev. Lett. **72**, 320 (1994); S.

Matarrese, S. Mollerach, and M. Bruni, Phys. Rev. D **58**, 043504 (1998); H. Noh and J. c. Hwang, Phys. Rev. D **69**, 104011 (2004); C. Carbone and S. Matarrese, Phys. Rev. D **71**, 043508 (2005); K. Nakamura, Prog. Theor. Phys. **117**, 17 (2007).

[11] S. Mollerach, D. Harari, and S. Matarrese, Phys. Rev. D **69**, 063002 (2004).

[12] K. N. Ananda, C. Clarkson, and D. Wands, Phys. Rev. D **75**, 123518 (2007).

[13] V. Mukhanov, *Physical Foundations of Cosmology* (Cambridge University Press, Cambridge, England, 2006); S. Dodelson, *Modern Cosmology* (Academic, New York, 2003).

[14] S. Matarrese, S. Mollerach, A. Notari, and A. Riotto, Phys. Rev. D **71**, 043502 (2005); R. Gopal and S. Sethi, Mon. Not. R. Astron. Soc. **363**, 521 (2005); K. Takahashi, K. Ichiki, H. Ohno, and H. Hanayama, Phys. Rev. Lett. **95**, 121301 (2005); K. Ichiki, K. Takahashi, H. Ohno, H. Hanayama, and N. Sugiyama, arXiv:astro-ph/0603631; K. Ichiki, K. Takahashi, N. Sugiyama, H. Hanayama, and H. Ohno, arXiv:astro-ph/0701329; T. Kobayashi, R. Maartens, T. Shiromizu, and K. Takahashi, Phys. Rev. D **75**, 103501 (2007).

[15] V. Acquaviva, N. Bartolo, S. Matarrese, and A. Riotto, Nucl. Phys. **B667**, 119 (2003).

[16] U. Seljak and M. Zaldarriaga, Astrophys. J. **469**, 437 (1996); http://www.cmbfast.org.

[17] A. Lewis and A. Challinor, http://camb.info.

[18] W. Hu, D. Scott, N. Sugiyama, and M. J. White, Phys. Rev. D **52**, 5498 (1995).

[19] S. Weinberg, Phys. Rev. D **69**, 023503 (2004); Y. Watanabe and E. Komatsu, Phys. Rev. D **73**, 123515 (2006).

[20] Latham Boyle, Ph.D. Thesis, Princeton University, 2006.

[21] T. L. Smith, M. Kamionkowski, and A. Cooray, Phys. Rev. D **73**, 023504 (2006).

[22] K. Enqvist and M. S. Sloth, Nucl. Phys. **B626**, 395 (2002); D. H. Lyth and D. Wands, Phys. Lett. B **524**, 5 (2002); T. Moroi and T. Takahashi, Phys. Lett. B **522**, 215 (2001); **539**, 303(E) (2002).

[23] N. Bartolo, S. Matarrese, A. Riotto, and A. Vaihkonen, arXiv:0705.4240 [Phys. Rev. D (to be published)].

[24] David Spergel and Lyman Page (private communication).